Low-Complexity Time-Domain DBP Based on Random Step-Size and Partitioned Quantization

Low-Complexity Time-Domain DBP Based on Random Step-Size and Partitioned Quantization

Celestino S. Martins, *Student Member, OSA*, Luca Bertignono, *Student Member, OSA*, Antonino Nespola, Andrea Carena, *Member, OSA, Member, IEEE*, Fernando P. Guiomar, *Member, OSA, Member, IEEE*, and Armando N. Pinto, *Senior Member, IEEE*

***Abstract*—We propose and experimentally validate a low complexity time-domain (TD) digital backpropagation (DBP) algorithm for fiber nonlinearity compensation, targeting an optimized hardware implementation. To counteract the coherent accumulation of numerical quantization errors between DBP steps, we propose a random step-size distribution along the optical link (with $\pm$5% interval around the optimal step-size). In addition, to further reduce the average quantization bit precision requirements, we propose a partitioned quantization technique, enabling to quantize the FIR filter tail coefficients with significantly lower precision. The proposed low complexity DBP algorithm is experimentally demonstrated over a 2592 km long-haul WDM transmission system with 21$\times$32 GBaud PM-16QAM optical channels. Employing the proposed step-size randomization together with dual-time-slot quantization we demonstrate penalty-free operation at an average of $\sim$4 bits per FIR coefficient, leading to a 60% complexity reduction when compared to the standard TD-DBP implementation.**

***Index Terms*—Optical fiber communications, nonlinear compensation, digital signal processing, digital backpropagation, FIR.**

I. Introduction

THE compensation of fiber nonlinear effects in the digital domain is a promising solution to increase the spectral efficiency (SE) and transmission reach in current optical transmission systems [1]. Among the large number of proposed digital signal processing (DSP) algorithms for nonlinearity compensation, digital backpropagation (DBP)-based techniques have been predominant [2]–[15]. The main challenge posed by these techniques arises from their high computational effort and power consumption requirements for hardware implementation [1]. These two aspects are fostering significant investigation efforts towards the development of advanced techniques with reduced complexity, aiming at an efficient hardware implementation and commercial deployment of DBP [3].

Reduced complexity DBP-based techniques for fiber nonlinearity compensation have been widely proposed in recent years, being predominantly implemented through computationally optimized versions of the well-known split-step Fourier method (SSFM) [4]–[7], which is based on the concatenation of a series of linear and nonlinear steps, thereby attempting to reverse the propagation of the transmitted signal over the optical link. Although several alternative DBP implementations have also gained considerable attention in recent years, such as those based on Volterra series nonlinear equalizers (VSNE) [8]–[10] and perturbation theory [11], [12], SSFM-based DBP remains as the most well-known and widely followed technique. Since its introduction for optical fiber communications [2], several important advances have been made to render SSFM-based DBP more computationally efficient. The vast majority of these efforts have been focused on the optimization of the implementation of the nonlinear step and on the development of advanced techniques to enable the use of fewer DBP steps. For this purpose, two main approaches have been recurrently addressed in the literature: i) the introduction of memory within the originally static SSFM nonlinear step, making use of several techniques such as low-pass filters [4], [5], logarithmic perturbation theory [6] or memory polynomials [7], and ii) the optimization of the nonlinear step position within the optical link [4]. Although these techniques have demonstrated significant improvement of computational efficiency through the reduction of the total number of DBP steps, it is important to note that the overall complexity associated with SSFM-based DBP is still largely dominated by the linear operator, which is commonly implemented in frequency-domain using fast Fourier transforms (FFT) and inverse FFTs (IFFT). Indeed, the nonlinear step in SSFM-based DBP is originally based on a simple memoryless power-dependent phase shift, which can be efficiently implemented through a low-order Taylor series expansion or even using look-up tables (LUTs) [16]. The main source of complexity is then originated by the recursive use of FFTs and IFFTs to implement the linear operator for each DBP step. Attempting to relax this complexity and facilitate hardware implementation, [13]–[15] have exploited full time-

This work has been partially funded by Fundação para a Ciência e a Tecnologia (FCT) through project UID/EEA/50008/2013 (action SoftTransceiver) and by the European Regional Development Fund (FEDER), through the Regional Operational Programme of Centre (CENTRO 2020) of the Portugal 2020 framework, Project ORCIP, CENTRO-01-0145-FEDER-022141. Celestino Martins acknowledges the financial support provided by FCT through the Ph.D. Grant PD/BD/113817/2015. Fernando P. Guiomar acknowledges the financial support provided by the European Commission through a Marie Skłodowska-Curie individual fellowship, project Flex-ON (653412).

Celestino S. Martins and Armando N. Pinto are with Department of Electronics, Telecommunications and Informatics, University of Aveiro and Instituto de Telecomunicações, 3810-193, Aveiro, Portugal, (e-mails: csmartins@av.it.pt and anp@ua.pt).

Andrea Carena and Luca Bertignono are with Dipartimento di Elettronica e Telecomunicazioni, Politecnico di Torino, Corso Duca degli Abruzzi, 24, 10129, Torino, Italy, (e-mail: andrea.carena@polito.it).

Antonino Nespola is with the Istituto Superiore Mario Boella, 10138, Torino, Italy (e-mail: nespola@ismb.it).

Fernando P. Guiomar was with Dipartimento di Elettronica e Telecomunicazioni, Politecnico di Torino. He is now with Instituto de Telecomunicações, Aveiro, Portugal, (e-mail: guiomar@av.it.pt).

domain (TD) DBP (TD-DBP), where the linear operator is implemented in TD through an efficient design of finite impulse response (FIR) filters. In this regard, [14], [15] have proposed advanced strategies based on coefficient quantization approaches to reduce the bit precision requirements of TD-DBP. These approaches have enabled penalty-free TD-DBP implementation, operating at 9-bit fixed-point precision [14], [15]. However, since the practical feasibility of DBP-TD-SSFM requires a low bit-precision implementation, it is imperative to further decrease these requirements, such that the implementation in a commercial hardware unit becomes feasible.

In this paper, we propose a novel TD-DBP approach based on step-size randomization and partitioned quantization techniques to reduce the requirements of hardware implementation of standard TD-DBP. The employment of a step-size randomization technique has enabled to improve the robustness of TD-DBP against numerical quantization errors on the FIR coefficients quantization, thereby allowing to reduce the required quantization bit precision for penalty-free operation. To further reduce the quantization bit precision we also propose to use a partitioned quantization scheme based on dual-time-slots, where a lower bit precision is allocated to the FIR filter tail coefficients. The proposed computationally efficient TD-DBP implementation is experimentally demonstrated over WDM long-haul transmission of a 21-channel PM-16QAM optical signal, enabling penalty-free TD-DBP operation at an average of $\sim$4 bits of precision for the FIR coefficients.

The rest of this paper is organized as follows. In section II, the concepts behind the proposed step-size randomization and partitioned quantization techniques are described. In Section III the performance and complexity of the proposed TD-DBP technique are experimentally assessed and discussed. Finally, in section IV, the main conclusions are presented.

II. Reduced Complexity Time-Domain Digital Backpropagation

In recent years the investigation of DBP-based techniques has been pushed towards the reduction of total number of operations (multiplications and additions) involved in an hardware implementation. Since the complexity of multiplications and additions is heavily related with the bit precision (number of bits) for the representation of their operands, the overall algorithm complexity is consequently highly driven by the minimum bit precision requirements for hardware implementation.

Before proceeding with the technical description of the proposed techniques for computational effort reduction, it is important to set a firm theoretical ground on the basic implementation of TD-DBP. The TD-DBP technique is based on the cascaded application of time-domain linear and nonlinear steps over the received optical signal, in order to estimate the corresponding transmitted signal. Considering a generic digitized optical field envelope, $A(t_n, z)$, defined at discrete time instants t_n and spatial position z, the linear TD-DBP operator applied over a step-size h, $\hat{D}_{\mathrm{h}}$, can be analytically written as,

$$\hat{D}_{\mathrm{h}}\Big(A(t_n, z)\Big) = A(t_n, z) * W_{\mathrm{CD}}(t_n, h_k), \tag{1}$$

where, $*$ represents the convolution operation and $W_{\mathrm{CD}}(t_n, h_k)$ is the complex-valued impulse response of the chromatic dispersion (CD) filter estimated over the step-size, h, which can be determined from the inverse Fourier transform of the CD compensation transfer function [17]. For simplicity, higher-order dispersion terms are commonly neglected when operating far away from the zero dispersion wavelength. Also note that, although it can be easily added to expression (1), the effect of signal attenuation can also be removed when TD-DBP is implemented with step-sizes equal or larger than the span length (and if the step-size is a multiple of the span length), which is a key requirement for a low-complexity DBP implementation. The time-domain implementation of the linear DBP operator as described by expression (1) can be achieved through the use of a FIR filter. The major drawback of this option is the $O(N^2)$ complexity associated with FIR filtering, as opposed to the $O(N\log(N))$ complexity of a frequency-domain FFT-based implementation. However, on the contrary of a frequency-domain implementation, whose major computational burden lies on the FFT processing itself (which is already very much optimized), in a time-domain implementation there is still significant room for computational efficiency optimization by taking advantage of the specificities of the case under study. A possible way of doing this is through the manipulation the W_{CD} coefficients in order to reduce complexity without sacrificing performance, a strategy that has been followed in several recent works [14], [15], [18].

In turn, the nonlinear DBP operator, $\hat{N}$, can be written as,

$$\hat{N}_{\mathrm{h}}\Big(A(t_n, z)\Big) = \exp\Big(-i\xi h_{\mathrm{eff}}\gamma|A(t_n, z)|^2\Big)A(t_n, z), \tag{2}$$

where γ is the Kerr nonlinear coefficient, $0 < \xi \leq 1$ is a free optimization parameter and h_{eff} is effective step-size for DBP, given by $h_{\mathrm{eff}} = (\exp(\alpha h) - 1)/\alpha$, with α being the fiber attenuation coefficient. Expression (2) highlights that, being based on a power-dependent phase-shift, the nonlinear DBP operator actually renders itself for a quite simple hardware implementation, namely resorting to the use of LUTs.

Cascading the linear and nonlinear operators defined above, each step of the TD-DBP algorithm can then be written as,

$$A(t_n, z-h) = \hat{N}_{\mathrm{h}}\left(\hat{D}_{\mathrm{h}}\Big(A(t_n, z)\Big)\right), \tag{3}$$

where, $A(t_n, z-h)$ is the compensated signal after one TD-DBP step, i.e. after backward propagation over a step-size h. The implementation of this standard TD-DBP algorithm with constant step-size is depicted in Fig. 1 a) for an hypothetic optical link composed of N_s identical fiber spans with ideal optical amplification (perfect recovery of optical power after each span). For simplicity, we consider a one-step per span TD-DBP implementation. Nevertheless, both the

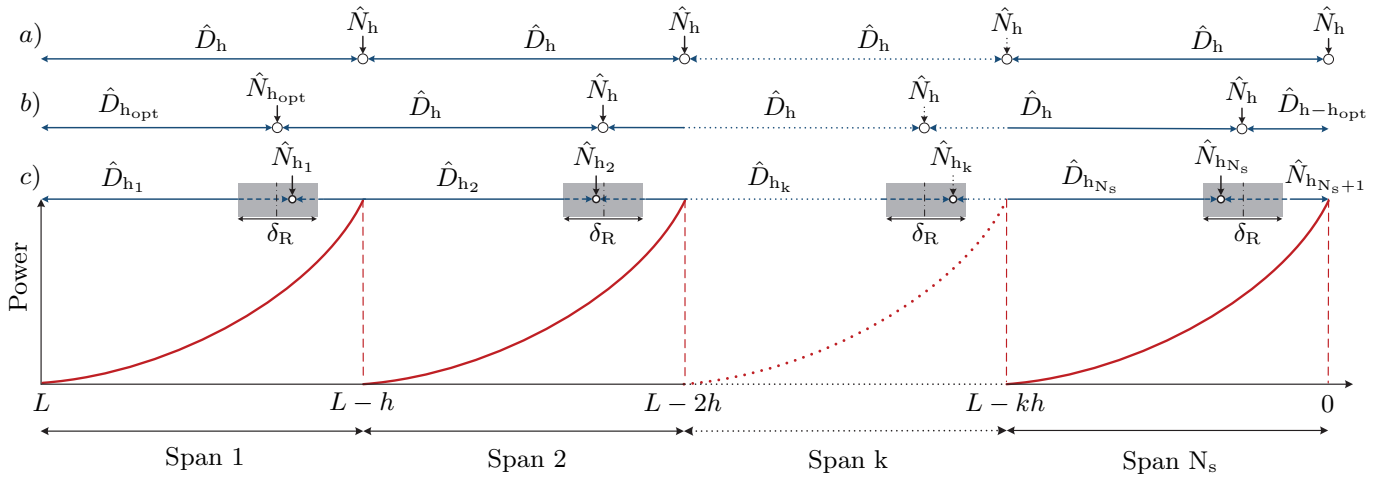

Fig. 1. An illustration of different one-step per span TD-DBP implementation schemes over an optical link composed of N_s identical fiber spans. a) standard TD-DBP with fixed step-size, h; b) fixed step-size TD-DBP with optimized positioning of the nonlinear operator, $h_{\rm opt}$; c) TD-DBP employing random step-size, h_k, (R-TD-DBP) with a randomization interval, $\delta_{\rm R}$, around the optimum position of the nonlinear operator, $h_{\rm opt}$. L is the total link length.

implementation diagram and the analytical formulation of (1)-(3) can be straightforwardly generalized for a multi-span per step scenario.

For the formulation of (3) we have assumed that the nonlinear DBP operator is applied after the linear operator, which is generally the best choice from the performance versus complexity point of view. Indeed, in Fig. 1 b) we show the implementation diagram of TD-DBP with optimized nonlinear step positioning for maximum performance. In general, for one-step per span implementation, it has been shown the optimum position of the $\hat{N}$ operator is at about $\sim$80% of the span length [4]. This implementation implies the use of an optimized step-size, $h_{\rm opt}$, for the first DBP step, followed by N_s-1 steps with a step-size equal to the span length and final linear-only DBP step with step-size $h-h_{\rm opt}$.

A. Step-Size Randomization

Given its cascaded structure, the performance of TD-DBP is highly sensitive to the bit precision of FIR coefficients employed in the computation of the linear step [14] due to the fast propagation of the quantization error, which tends to accumulate coherently if all FIR coefficients for each DBP step are identical. In order to partially counteract this effect, [14] has proposed dithering of the FIR coefficients, while [15] has proposed joint optimization of FIR filter pairs. In this work, we propose a simpler approach to increase the robustness of TD-DBP against quantization noise, which is based on the randomization of the DBP step-size (R-TD-DBP), thereby enabling to partially decorrelate the quantization error across different DBP steps without the need for introducing dithering noise or performing complex joint FIR optimization. The primary idea behind this concept is to randomize the step-size, h, in TD-DBP over each step along all the fiber spans, such that a different step-size, h, is applied for each step. This in turn, implies that a slightly different amount of dispersion is compensated at each DBP step, resulting in the use of different sets of FIR filter coefficients. Given that the FIR coefficients are different for each DBP step, the generated quantization noises become partially decorrelated, enabling a quasi incoherent accumulation of quantization noise across DBP steps. Thereby, the minimum bit precision requirements of TD-DBP can be substantially alleviated, an effect that becomes more prominent as the number of steps increases.

The concept of step-size randomization is shown in Fig. 1 c), which can be directly compared to the standard fixed step-size TD-DBP with optimized positioning of the nonlinear step. As evidenced by Fig. 1 c), the proposed R-TD-DBP technique makes use of different step-sizes, h_k, in each DBP step for the computation of the linear and nonlinear steps. The step-size of the k-th R-TD-DBP step, h_k, is randomly chosen inside an interval $\delta_{\rm R}$, which corresponds to a segment of the fiber span, $\delta_{\rm R} = Rh$, where R is the interval of randomization in percentage. Note that the chosen value of R will play a critical role on the complexity versus performance trade-off of R-TD-DBP: while on one hand, large R ensures an effective decorrelation of the FIR filters, on the other hand it will also detune the optimum position of the $\hat{N}$ operator. Further details on this issue are provided in section III. The random step-size, h_k, across all R-TD-DBP steps can be defined as,

$$h_k = \begin{cases} r_1 h_{\rm opt}, & k=1 \\ h + h_{\rm opt}(r_k - r_{k-1}), & 1 < k \leq N_{\rm s} \\ h - r_{N_{\rm s}} h_{\rm opt}, & k = N_{\rm s}+1 \end{cases} \tag{4}$$

where, r_k is a random variable that defines the percentage of the deviation of h_k with respect to the optimum position, $h_{\rm opt}$, following an uniform distribution,

$$r_k \sim \mathcal{U}\left(1-\frac{R}{2}, 1+\frac{R}{2}\right). \tag{5}$$

B. Partitioned Quantization

In Fig. 2 we illustrate an example of the CD compensation filter impulse response over a step-size h equal to the span length, as required by a one-step per span TD-DBP

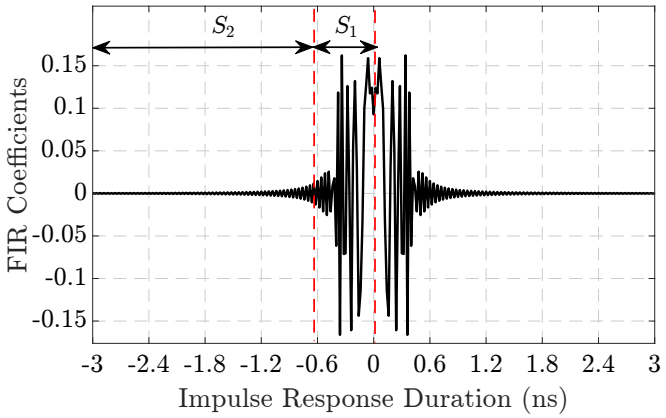

Fig. 2. Dual-time-slot quantization process applied to the real part of the FIR coefficients for CD compensation inside one TD-DBP step. The FIR coefficients are partitioned into two time-slots, S_1 and S_2.

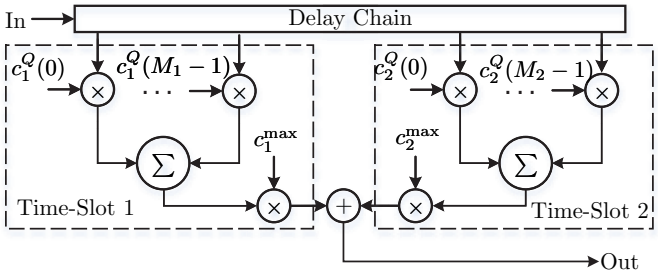

Fig. 3. FIR filter implementation for a dual-time-slot quantization process. The multiplication by $c_1^{\max}$ and $c_2^{\max}$ accounts for the renormalization process of FIR coefficients after quantization.

implementation. From a closer inspection of Fig. 2, we can observe that the distribution of coefficients of the FIR filter enables its division into multiple rather distinct partition, with each partition comprising a given range of amplitude values. Thus, an efficient quantization of the FIR filter coefficients would benefit from a separate treatment of each partition. In this paper we have designated each partition as a time-slot. Based on this observation, we propose a dual-time-slots (DS) quantization process, where the filter impulse response is partitioned into two time-slots and the quantization process is applied to each time-slot separately with a different number of levels or with a different quantization intervals. Each time-slot quantization can be performed according to,

$$c_j^Q(k) = c_j^{\max} \frac{\left\lfloor \Delta_j \frac{c_j(k)}{c_j^{\max}} \right\rceil}{\Delta_j}, \; k = 0, ..., M_j - 1, \qquad (6)$$

where $j = 1, 2$ represents the index of the time-slot S_j, Δ_j is the quantization factor per time-slot, $c_j(k)$ are the complex-valued FIR coefficients within S_j and c_j^Q are the corresponding quantized FIR coefficients. The quantization process is applied to all M_j FIR coefficients within each time-slot S_j. The quantization process itself is applied by a nearest integer operation, $\lfloor \cdot \rceil$, after normalizing the FIR coefficients by the maximum value among the real and imaginary parts of the FIR coefficients within each time-slot, $c_j^{\max}$, such that $c_j^{\max} = \max(|c_j^r(k)|, |c_j^i(k)|$, where $c_j^r(k)$ and $c_j^i(k)$ are the real and imaginary parts of $c_j(k)$. Benefiting from the rather different amplitude ranges of FIR coefficients within each time-slot, we can adjust the quantization factor, Δ_j, on a per time-slot basis. In general, time-slots with wider amplitude range require higher values of Δ for an accurate quantization, whereas time-slots with lower amplitude range may favor the use of lower values of Δ. In Fig. 2 we consider a dual-time-slot approach, where the FIR coefficients are divided into two time-slots: i) the central part of the FIR (slot S_1), whose coefficients vary over a wide range of values, and ii) the FIR tail (slot S_2), where the coefficients vary within a much more restricted range. The optimum values of Δ_j and number of coefficients per time-slot, M_j, can be optimized numerically. According to the distribution of FIR coefficients shown in Fig. 2, we may expect that the use of this dual-time-slot quantization approach will significantly reduce the bit precision requirements in time-slot S_2, thus contributing to lower the total average bit precision weighted over the two time-slots. It should be also noted that, to take advantage of the FIR filter symmetry, we consider as well a folded delay line FIR structure, enabling to half the number of effective FIR coefficients [18].

Due to the different normalization factors per time-slot, $c_j^{\max}$, it results that the FIR impulse response becomes affected by a differential gain between time-slots. For a correct compensation of CD, it is then mandatory to compensate for this differential gain within the filtering process. This can be done by slightly modifying the FIR filter structure, as shown in Fig. 3. Taking advantage of the fact that the normalization factor, $c_j^{\max}$, is common to all FIR coefficients inside each time-slot, the renormalization can then be applied after summing up all their contributions, thus requiring only a single extra real multiplication by $c_j^{\max}$ per time slot. Using a dual-time-slot approach together with an FIR filter composed of several tens of coefficients, the extra complexity required by this operation is very residual and thus can be neglected.

It is worth to highlight that the proposed dual-time-slot quantization approach can be easily extended to a multi-time-slot quantization, by partitioning the FIR coefficients into any given number of time-slots. In general, the use of a larger number of partitions will enable further gains in quantization precision, at the expense of an increasing complexity on the renormalization stage. For each case under study, there is an optimized tradeoff between these two aspects that minimizes the overall computational effort. However, in order to keep a simple filter structure and to simplify the overall analysis, in this paper we stick to the use of a dual-time-slot quantization process, which we identify as being an adequate solution to significantly reduce the TD-DBP complexity.

III. Experimental Results

In this section, we provide the experimental validation of the proposed techniques considering the laboratorial setup depicted in the Fig. 4. At the transmitter-side 21 channels, composed of channel under test (CUT), odd carriers and even carriers, are generated each at 32 GBaud. An external

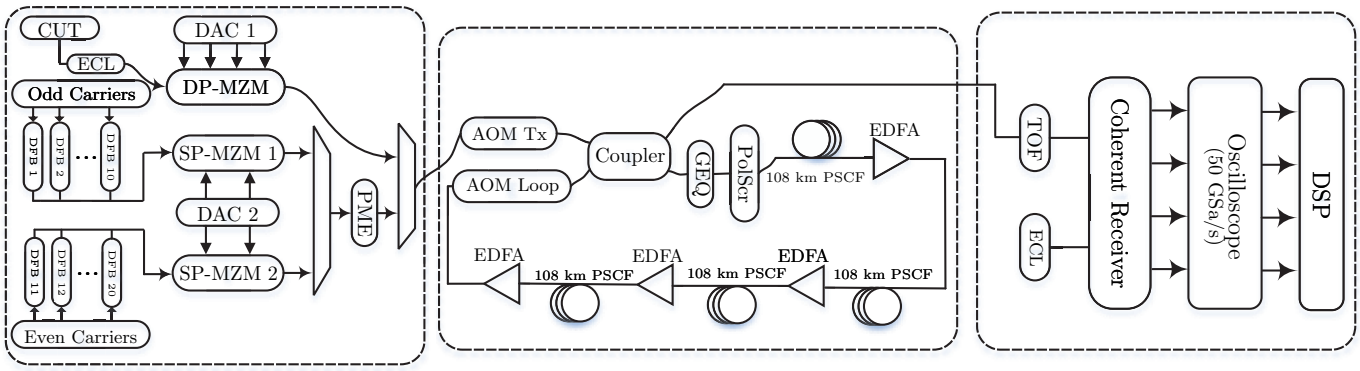

Fig. 4. Experimental setup of 21×32 GBaud WDM PM-16QAM transmission system. Recirculating loop composed of 4×108 km span of pure silica core fiber (PSCF). CUT - channel under test; ECL - external cavity lasers; DAC - digital to analog converter; DP-MZM - dual-polarization Mach-Zehnder modulator; DFB - distributed feedback; SP-MZM - single-polarization MZM; PME - polarization multiplexing emulator; AOMs - acousto-optical modulators; EDFAs - erbium-doped fiber amplifiers; GEQ - gain-equalizer; PolScr - polarization scrambler; TOF - tunable optical filter.

cavity laser (ECL) is utilized to modulate the CUT, whose in-phase (I) and quadrature (Q) components are generated by a 64 GSa/s digital to analog converter (DAC) and fed into the dual-polarization Mach-Zehnder modulator (DP-MZM) for optical modulation. The remaining 20 interferer channels are modulated by distributed feedback (DFB) lasers arranged in 10 odd and even carriers. A 4-port DAC is utilized to generate the I and Q components, which feed two single-polarization MZM (SP-MZM), corresponding to odd and even carriers, for optical modulation. Then, a polarization multiplexing emulator (PME) is utilized to perform optical polarization multiplexing for the interferer channels. The transmission link comprises a recirculating-loop, which is controlled by acousto-optical modulators (AOMs) and is composed of four spans of pure silica core fiber (PSCF) with average length of 108 km, characterized by $\alpha = 0.16$ dB/km and dispersion, $D = 20.17$ ps/(nm $\cdot$ km). Erbium-doped fiber amplifiers (EDFAs) with 5.4-dB noise figure are utilized to recover the loss and a gain-equalizer (GEQ) followed by a polarization scrambler (PolScr) are utilized every loop to flatten the optical gain and to statistically average the polarization effects. At the receiver side, the CUT is filtered by a tunable optical filter (TOF), which is then coherently detected utilizing a second ECL as local oscillator. Then, the electrical signal is sampled by a 50 GSa/s oscilloscope with 33 GHz electrical bandwidth and followed by offline post-processing. The DSP comprises linear (CDE) or nonlinear (TD-DBP) compensation, adaptive equalization, carrier recovery and finally SNR estimation from the equalized signal constellation. As for nonlinear compensation, we have applied both the standard TD-DBP and our proposed techniques.

A. Preliminary Optimization of Standard TD-DBP

We start our analysis with the optimization of the main nonlinear compensation parameters, such as launched power, number of steps per span, N_{steps}, and position of the nonlinear operator. Furthermore, the number of FIR filter coefficients is optimized such that penalty-free linear equalization is ensured with minimum complexity [17]. As for nomenclature, we have defined TD-DBP$_{N_{\text{steps}}}$ as the standard TD-DBP applied with

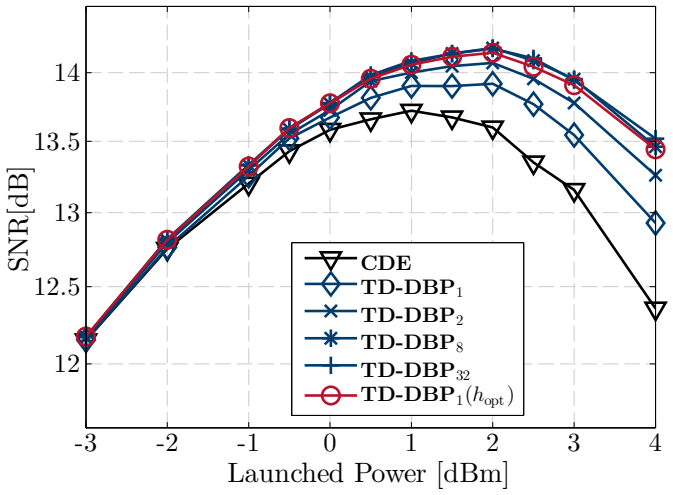

Fig. 5. SNR as a function of launched power considering different number of steps per span, N_{steps}, for a propagating distance of 2592 km. Optimizing the position of nonlinear operator, curve TD-DBP$_1(h_{\text{opt}})$, allows to achieve the maximum performance with only 1-step per span.

N_{steps} per span and TD-DBP$_{N_{\text{steps}}}(h_{\text{opt}})$ as the TD-DBP$_{N_{\text{steps}}}$ algorithm with optimized positioning of the nonlinear operator. In this optimization the floating-point bit precision for the FIR filter coefficients is considered. In this regard, Fig. 5 shows the evaluation of performance for these different TD-DBP algorithms in terms of estimated SNR of the equalized constellation as a function of input power, and considering different number of steps per span. The transmission distance under test is 2592 km (24 fiber spans). We can observe that the maximum performance is achieved by employing 8-steps per span, TD-DBP$_8$, yielding an optimum launched power of 2 dBm,$\sim$1 dB higher than with CD equalization (CDE) only, and an SNR gain over CDE of $\sim$0.5 dB. To try to reduce the TD-DBP step-size requirements, we have optimized the position of nonlinear operator [19], which was found at $\sim$80% of the span length for $N_{\text{steps}} = 1$, corresponding to h_{opt} of $\sim$86.4 km. The obtained results confirm that, by simply optimizing the position of nonlinear operator, we can operate

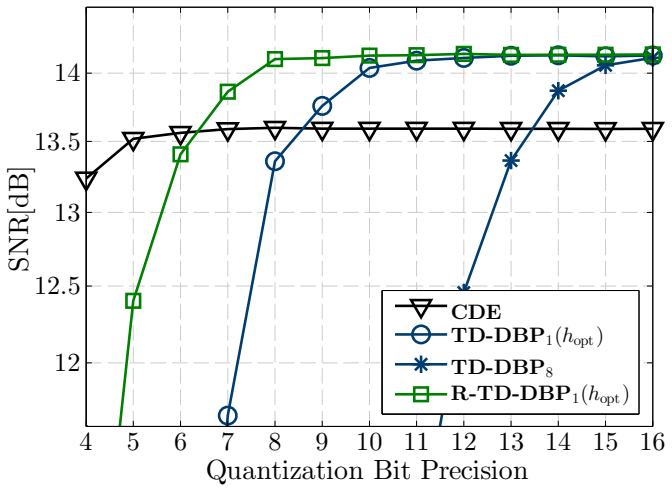

Fig. 6. SNR of the equalized signal after TD-DBP as a function of the number of bits for FIR coefficient quantization, considering different step-size configurations. The propagation distance is 2592 km and the launched power is 2 dBm. R-TD-DBP$_1(h_{\rm opt})$ is applied with a randomization interval of $R = 10\%$ of the span length.

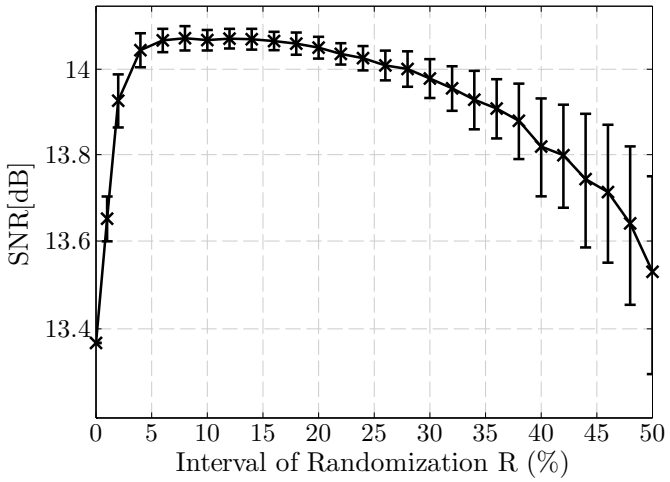

Fig. 7. SNR after applying R-TD-DBP$_1(h_{\rm opt})$ as a function of the randomization interval, R, in percentage of the span length. The optimization is performed for 8 bits precision FIR coefficients. The propagation distance is 2592 km and the launched power is 2 dBm. The solid line and markers indicate the average SNR obtained from 100 independent realization of R-TD-DBP. The corresponding standard deviation is indicated by the error bars.

at 1-step per span with roughly the same accuracy as an 8-steps per span TD-DBP. The optimization of the nonlinear operator position for 2-steps per span has been also performed, however, negligible improvement has been achieved. These simple optimizations, well known from the literature, are the first key step for a preliminary reduction of DBP complexity in this work. Our proposed techniques will now operate over the optimized TD-DBP$_1(h_{\rm opt})$.

B. Step-Size Randomization

We now proceed with the investigation on the quantization bit precision requirements for the FIR filters employed in the linear operator of TD-DBP. To this end, we evaluate the performance of TD-DBP algorithms considering different quantization accuracy ranging from low precision (4 bits) to high precision (16 bits), and using different TD-DBP step-sizes. The corresponding results are shown in Fig. 6, where we can note that as the step-size increases (decreasing $N_{\rm steps}$) the required bit precision for the FIR filters to achieve the maximum performance also decreases. Indeed, a reduction of 4 bits is achieved by simply considering TD-DBP$_1(h_{\rm opt})$ (requiring 11 bits) instead of the standard TD-DBP$_8$ (requiring 15 bits). This achievement can be justified by the fact that the quantization errors are propagated over a lower number of steps, thus reducing the error accumulation. However, the 11-bits quantization achieved by TD-DBP$_1(h_{\rm opt})$ still remains a quite demanding hardware requirement.

Aiming at a further decrease of bit precision requirements, we proceed with the experimental assessment of R-TD-DBP. For the employment of this technique, first we have optimized the randomization interval, $\delta_{\rm R}$, illustrated in Fig. 1. To that purpose, we have chosen a wide set of different randomization intervals ranging from $R = 0$ (deterministic) to $R = 0.5$, and we have performed 100 independent realizations of R-TD-DBP employing uncorrelated random variables r_k (see eq. (5)) to determine the step-size, h_k, per R-TD-DBP step. In addition, we consider an 8-bits precision for the quantization of the FIR filter coefficients. To analyze this effect, we operate at a propagation distance of 2592 km and an optimum power of 2 dBm, corresponding to the maximum performance registered in Fig. 5. Besides the average SNR obtained from all 100 independent R-TD-DBP realizations, we also indicate the corresponding standard deviation in Fig. 7, in the form of error bars. The obtained results are shown in Fig. 7, which clearly puts in evidence the benefit of using a randomization interval in R-TD-DBP. Note that, with $R = 0$ the maximum SNR of $\sim$14.2 dB obtained in Fig. 5 (where a floating point precision was considered) drops down to approximately 13.4 dB, corresponding to a loss of performance of about 0.8 dB, which would make the 8-bits implementation of TD-DBP perform even worse than CDE. On the other hand, if the randomization interval is too wide, we have found that SNR performance again tends to decrease, due to the random displacement on the optimum position of the nonlinear operator. For the current case study, we have found that a randomization interval of 10% of the span length ($\delta_{\rm R}$ =10.8 km) provides a near optimum performance. This means that, in the following results, R-TD-DBP operates with a step-size that is randomly selected within ± 5.4 km of the optimum step-size of TD-DBP$_1(h_{\rm opt})$. The performance of R-TD-DBP$_1(h_{\rm opt})$ as a function of quantization bit precision is then shown in Fig. 6, confirming the ability for penalty-free operation with 8-bits quantization of the FIR coefficients, a 3-bit reduction with respect to the benchmark TD-DBP$_1(h_{\rm opt})$.

C. Dual-Time-Slot Quantization

To further relax the required quantization bit precision, we now introduce the dual-time-slot (DS) quantization approach over R-TD-DBP, aiming at a more efficient quantization of the FIR tail coefficients, such that the overall average bit

precision can be reduced below the 8-bits limit found above. In this regard, we have fixed the bit precision of time-slot S_1 (central part of the FIR) to 8 bits, corresponding to the minimum precision requirements obtained from Fig. 6. Since time-slot S_1 comprises the range of FIR coefficients that require higher bit precision, it is also essential to minimize the length of time-slot S_1, M_1, while maximizing the length of time-slot S_2, while achieving penalty-free operation of DS-R-TD-DBP. We have conducted this study by varying the number of bits for the quantization of FIR coefficients (< 8) allocated to time-slot S_2 and we identify the maximum number coefficients that can be allocated to this time-slot (M_2) while achieving a penalty-free operation, corresponding to an SNR gain ($\mathrm{SNR_{gain}}$) $\geq$0.5 dB over CDE. The obtained results are presented in Fig. 8 for an FIR filter with symmetric length of 151 taps, which corresponds to the optimized length for penalty-free CD compensation. In general, we can observe that as we lower the quantization bit precision in time-slot S_2 also the partitioning point between slots tends to shift towards the tail of the FIR filter, i.e, M_2 tends to decrease while M_1 increases proportionally. This is the expected result since as we increase M_2 the required bit-precision in time-slot S_2 also tends to increase in order track the larger amplitude variation of FIR coefficients. In addition, Fig. 8 also indicates the average number of bits calculated over the two time-slots of FIR coefficients (S_1 and S_2), as a function of bit precision in time-slot S_2. This average can be estimated by weighting the bit precision in time-slot S_1 and S_2 by their respective lengths, M_1 and M_2. An optimum operating point is found at 2 bit precision for time-slot S_2. For this particular case, around 65% of FIR coefficients are represented with 2 bits (S_2), whereas only the remaining 35% operates with 8 bits precision (S_1), therefore, providing an average bit precision of $\sim$4.1 bits over the two time-slots of the FIR filter. This represents a bit precision reduction of more than 60% and 70% with respect to the 11 bits required by TD-DBP$_1(h_{\mathrm{opt}})$ and the 15 bits required by TD-DBP$_8$, respectively. It is also worth noting that when 0 bit precision (all coefficients are interpreted as zeros) is applied to S_2, no coefficients can be allocated to that time-slot, confirming that the impulse response of the FIR could not be further truncated below the considered 151 taps.

Taking into account the main parameters that impact the complexity of DBP-based techniques, we can define the overall complexity as being proportional to the number of steps per span, N_{steps}, number of FIR coefficients, N_{taps}, and bit precision for the FIR coefficients, N_{bits}, ($\propto N_{\mathrm{steps}} N_{\mathrm{taps}} N_{\mathrm{bits}}$). Based on this proportionality it becomes clear that a considerable reduction in the algorithm complexity can be obtained by simply reducing the bit precision associated to the FIR coefficients, thereby evidencing the impact of the proposed techniques on the overall algorithm complexity reduction. The proposed random step-size and partitioned quantization techniques can be applied to any DBP-based techniques implemented in time-domain, where the quantization process is exploited, leading to a significant complexity reduction.

To provide an extended analysis of the proposed technique in comparison with standard TD-DBP, we have evaluated the maximum reach for the system under test, by varying the number of recirculating loops from 1 to 20 and launched power from -3 dBm to 4 dBm. Fig. 9 describes the obtained results for CDE, TD-DBP$_8$ and DS-R-TD-DBP$_1(h_{\mathrm{opt}})$, indicating that the nonlinear compensation algorithms provide a maximum reach increase of $\sim$15% with respect to the CDE. In addition, we can note a good agreement between the maximum performance algorithm, TD-DBP$_8$, and the proposed low complexity algorithm, DS-R-TD-DBP$_1(h_{\mathrm{opt}})$, demonstrating that DS-R-TD-DBP concept can be applied over a wide range of propagation distances and launched powers.

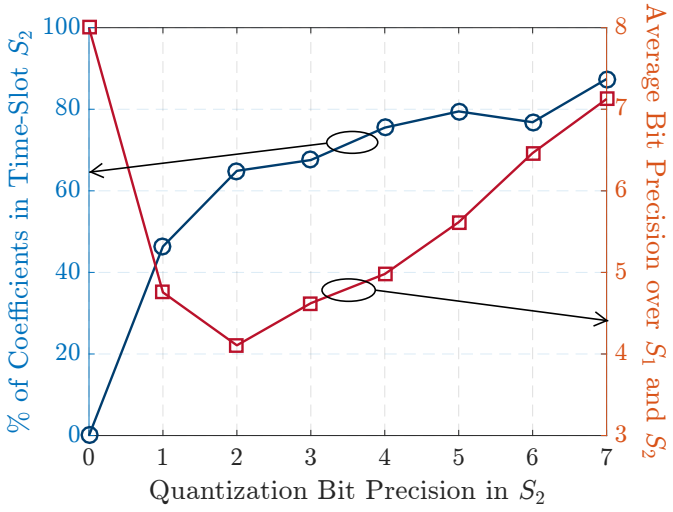

Fig. 8. Optimization of dual-time-slot quantization to minimize the weighted average bit precision requirements over time-slots S_1 and S_2. The bit precision for S_2 is optimized after fixing 8 bits for S_1. Left-hand axis accounts for the maximum % of coefficients in S_2 that preserves $\mathrm{SNR_{gain}}$ > 0.5 dB, whereas the right-hand axis corresponds to the average overall bit precision weighted over the number of coefficients in S_1 and S_2.

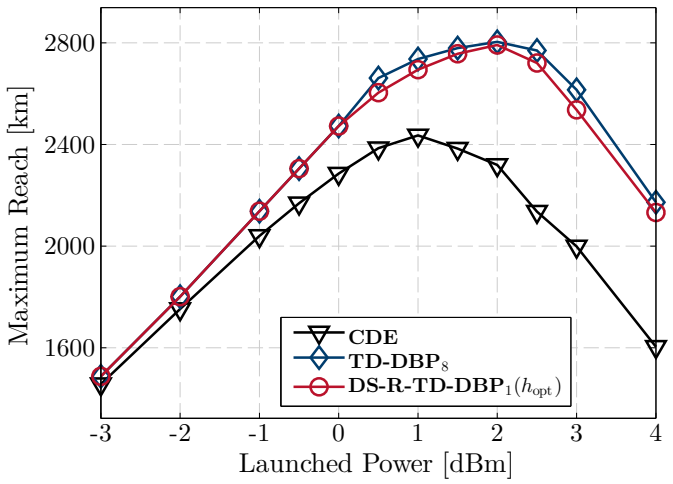

Fig. 9. Maximum reach achieved for CDE, TD-DBP$_8$ and DS-R-TD-DBP$_1(h_{\mathrm{opt}})$. Employing reduced complexity DS-R-TD-DBP(h_{opt}) with one step per span, we can achieve the same maximum reach as standard TD-DBP using 8-steps per span

IV. Conclusions

We have proposed a low complexity fully time-domain DBP approach based on step-size randomization and dual-time-slot quantization. The use of a step-size randomly distributed around 10% of the span length was shown to significantly enhance the TD-DBP robustness against quantization noise from the FIR filter coefficients, enabling penalty-free operation with only 8 bits per coefficient, which is compared to the 11 bits required by standard TD-DBP. To further reduce the quantization bit precision requirements, a partitioned quantization technique is proposed, where the filter impulse response is divided into two time-slots that are quantized separately. By doing so, we have experimentally demonstrated penalty-free operation allocating only 2 bits for the quantization of 65% of all FIR coefficients. This corresponds to an average number of ~ 4 bits per FIR coefficient, providing around 60% reduction for quantization bit precision requirements with respect to the standard TD-DBP. The proposed techniques has been experimentally demonstrated in a 21×32 GBd WDM PM-16QAM transmission system, enabling to increase the maximum reach by $\sim$15% when compared with standalone CDE.

References

[1] J. C. Cartledge, F. P. Guiomar, F. R. Kschischang, G. Liga, and M. P. Yankov, "Digital signal processing for fiber nonlinearities," *Opt. Express*, vol. 25, no. 3, pp. 1916–1936, Feb 2017.

[2] E. Ip and J. M. Kahn, "Compensation of dispersion and nonlinear impairments using digital backpropagation," *J. Lightw. Technol.*, vol. 26, no. 20, pp. 3416–3425, 2008.

[3] H. Nakashima, T. Oyama, C. Ohshima, Y. Akiyama, T. Hoshida, and Z. Tao, "Digital nonlinear compensation technologies in coherent optical communication systems," in *Optical Fiber Communication Conference*. Optical Society of America, 2017, p. W1G.5.

[4] L. B. Du and A. J. Lowery, "Improved single channel backpropagation for intra-channel fiber nonlinearity compensation in long-haul optical communication systems," *Opt. Express*, vol. 18, no. 16, pp. 17 075–17 088, Aug 2010.

[5] D. Rafique, J. Zhao, and A. D. Ellis, "Digital back-propagation for spectrally efficient WDM 112 Gbit/s PM m-ary QAM transmission," *Opt. Express*, vol. 19, no. 6, pp. 5219–5224, Mar 2011.

[6] M. Secondini, S. Rommel, G. Meloni, F. Fresi, E. Forestieri, and L. Potì, "Single-step digital backpropagation for nonlinearity mitigation," *Photonic Network Communications*, vol. 31, no. 3, pp. 493–502, 2016.

[7] J. Gonçalves, C. S. Martins, F. P. Guiomar, T. R. Cunha, J. C. Pedro, A. N. Pinto, and P. M. Lavrador, "Nonlinear compensation with DBP aided by a memory polynomial," *Opt. Express*, vol. 24, no. 26, pp. 30 309–30 316, Dec 2016.

[8] G. Shulkind and M. Nazarathy, "Nonlinear digital back propagation compensator for coherent optical OFDM based on factorizing the Volterra series transfer function," *Opt. Express*, vol. 21, no. 11, pp. 13 145–13 161, Jun 2013.

[9] F. P. Guiomar, S. B. Amado, C. S. Martins, and A. N. Pinto, "Parallel split-step method for digital backpropagation," in *Optical Fiber Communication Conference*. Optical Society of America, 2015, p. Th2A.28.

[10] S. B. Amado, F. P. Guiomar, N. J. Muga, R. M. Ferreira, J. D. Reis, S. M. Rossi, A. Chiuchiarelli, J. R. F. Oliveira, A. L. Teixeira, and A. N. Pinto, "Low complexity advanced DBP algorithms for ultra-long-haul 400G transmission systems," *Journal of Lightwave Technology*, vol. 34, no. 8, pp. 1793–1799, April 2016.

[11] L. Xiang, P. Harper, and X. Zhang, "Advanced perturbation technique for digital backward propagation in WDM systems," *Opt. Express*, vol. 21, no. 11, pp. 13 607–13 616, Jun 2013.

[12] X. Liang and S. Kumar, "Correlated digital back propagation based on perturbation theory," *Opt. Express*, vol. 23, no. 11, pp. 14 655–14 665, Jun 2015.

[13] X. Zhou, J. Yu, M.-F. Huang, Y. Shao, T. Wang, P. Magill, M. Cvijetic, L. Nelson, M. Birk, G. Zhang, S. Ten, H. B. Matthew, and S. K. Mishra, "32Tb/s (320×114Gb/s) PDM-RZ-8QAM transmission over 580km of SMF-28 ultra-low-loss fiber," in *Proc. Optical Fiber Communication Conf. and Exposition (OFC)*, 2009.

[14] C. Fougstedt, L. Svensson, M. Mazur, M. Karlsson, and P. Larsson-Edefors, "Time-domain digital back propagation: algorithm and finite-precision implementation aspects," in *Optical Fiber Communication Conference*. Optical Society of America, 2017, p. W1G.4.

[15] C. Fougstedt, M. Mazur, L. Svensson, H. Eliasson, M. Karlsson, and P. Larsson-Edefors, "Finite-precision optimization of time-domain digital back propagation by inter-symbol interference minimization," in *Proc.European Conf. Optical Communication (ECOC)*, paper W.1.D.2, 2017.

[16] E. F. Mateo, F. Yaman, and G. Li, "Efficient compensation of inter-channel nonlinear effects via digital backward propagation in WDM optical transmission," *Opt. Express*, vol. 18, no. 14, pp. 15 144–15 154, Jul 2010.

[17] T. Xu, G. Jacobsen, S. Popov, J. Li, E. Vanin, K. Wang, A. T. Friberg, and Y. Zhang, "Chromatic dispersion compensation in coherent transmission system using digital filters," *Opt. Express*, vol. 18, no. 15, pp. 16 243–16 257, Jul 2010.

[18] C. S. Martins, F. P. Guiomar, S. B. Amado, R. M. Ferreira, S. Ziaie, A. Shahpari, A. L. Teixeira, and A. N. Pinto, "Distributive FIR-based chromatic dispersion equalization for coherent receivers," *Journal of Lightwave Technology*, vol. 34, no. 21, pp. 5023–5032, Nov 2016.

[19] C. Y. Lin, M. Holtmannspoetter, M. R. Asif, and B. Schmauss, "Compensation of transmission impairments by digital backward propagation for different link designs," in *36th European Conference and Exhibition on Optical Communication*, Sept 2010, pp. 1–3.